DESIGN AND TESTING OF AN AEROELASTICALLY TAILORED WING UNDER MANOEUVRE LOADING

Noud P.M Werter[1], Jurij Sodja[1], and Roeland De Breuker[1]

[1] Delft University of Technology
Kluyverweg 1, 2629 HS Delft,
The Netherlands
N.P.M.Werter@tudelft.nl

Keywords: aeroelasticity, aeroelastic tailoring, load alleviation, design, experiment.

Abstract: The design methodology and testing of an aeroelastically tailored wing subjected to manoeuvre loads is presented in this paper. The wing is designed using an aeroelastic analysis tool that is composed of a closely coupled nonlinear beam model and a vortex lattice aerodynamic model. The globally convergent method of moving asymptotes is used to derive an optimal layup design for a constant and variable stiffness wing. In addition a quasi-isotropic wing is designed in order to provide baseline reference data. Each wing design is manufactured and tested in the wind tunnel. Lift and root bending moment coefficient and wing deformation have been measured during the test. Measurements were used to validate the numerical results. The agreement between the numerical results and measurements was very good. The comparison yielded an average absolute difference of less than 10% in the case of lift and root bending moment coefficient and an average absolute difference of less than 5% in the case of the wing tip out-of-plane deformation.

1 INTRODUCTION

Composite materials are gaining more and more interest in the aerospace industry. Composite materials have two main advantages: (1) they have favourable specific properties compared to metals and (2) they have the ability to tailor the material properties according to the structural needs. This second property allows for aeroelastic tailoring, which has been nicely defined by Shirk et al. [1] as:

"the embodiment of directional stiffness into an aircraft structural design to control aeroelastic deformation, static or dynamic, in such a fashion as to affect the aerodynamic and structural performance of that aircraft in a beneficial way".

Aeroelastic tailoring has been researched extensively over the years. A summary of early research on aeroelastic tailoring of swept and unswept wings has been written by Shirk et al. [1]. More recently Qin et al. [2], [3] have done research on assessing the aeroelastic instability of composite thin-walled beams to investigate the effect of aeroelastic tailoring. Furthermore, several papers on the use of aeroelastic tailoring in general and the potential benefits it has, have been written recently by Weisshaar [4]–[7]. More specific research on the use of aeroelastic tailoring has been done to minimize structural weight [8]–[12], maximize flutter speed [10], [11], [13]–[16] optimise the gust response characteristics of wings, [17], [18] and the effect of tow-steered composites on wing aeroelastic characteristics [19]. An example of the use of aeroelastic tailoring in non-aerospace applications is the research by Thuwis et al. [20] on the use of aeroelastic tailoring on the rear wing of a F1 car.

As can be seen, substantial research is done on the potential benefits of aeroelastic tailoring; however, very little experimental validation is available. Some experimental work is described in the overview paper by Shirk et al., but it is interesting to note that recently no experimental validation data has become available to validate current aeroelastic models and also show the practical use of aeroelastic tailoring for load alleviation. Moreover, no experimental data is available on the strains in composite wing structures under aerodynamic loading. Therefore this paper presents an experimental study into the use of aeroelastic tailoring for manoeuvre load alleviation.

First, an overview of the aeroelastic analysis module used to analyse and design the aeroelastically tailored wings is given in section 2. Next the optimisation procedure used to design the wings is explained in section 3, followed by the outline of the actual design of the wings in section 4. Wing manufacturing and the experimental setup are described in section 5. Finally numerical and experimental results are presented and discussed in section 6. The most important findings and observations are summed up in section 7.

2 AEROELASTIC ANALYSIS MODULE

This section provides an overview of the static aeroelastic analysis that was used to analyse the aeroelastic performance of the composite wing considered. The static aeroelastic model is based on Werter et al. [21] Figure 1 shows a schematic of the static aeroelastic analysis and the different modules it consists of.

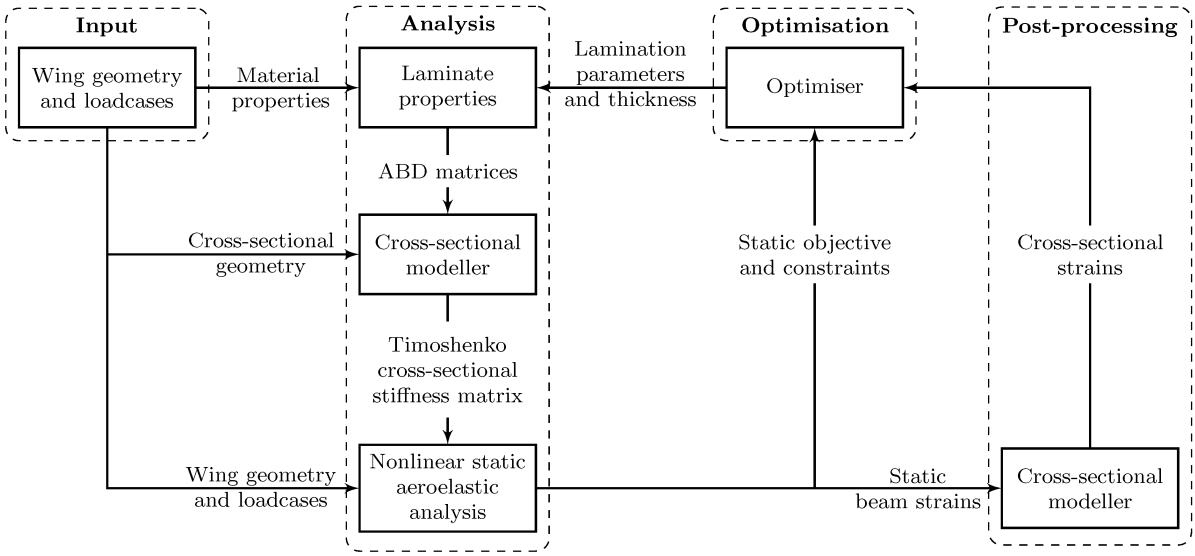

Figure 1: Static aeroelastic analysis module

Since an aeroelastic optimisation needs to be done, one of the key requirements of the framework is computational efficiency. For this purpose, the three-dimensional wing geometry is split in several spanwise sections, each having its own skin laminate distribution throughout the wing cross-section. These laminates are described using lamination parameters and the laminate thickness, since these define any composite laminate using a fixed number of continuous design variables, which allows for the use of more efficient optimisers.

The aeroelastic analysis and optimisation loop starts with the definition of the wing geometry and load cases as inputs to the loop. Next, the composite laminate properties that are used for the wing skins and spars are determined based on the material properties given as input and

the lamination parameters and thicknesses generated by the optimiser. In order to generate the beam model, these laminate properties, together with the cross-sectional geometry, are used to generate the Timoshenko cross-sectional stiffness matrix with respect to the beam reference axis, using the cross-sectional modeller developed by Ferede et al. [22].

As a third step, a geometrically nonlinear static aeroelastic analysis is carried out to obtain the nonlinear static displacement field of the aircraft for the various load cases. The static aeroelastic model couples a geometrically nonlinear Timoshenko beam model based on the co-rotational formulation to a vortex lattice aerodynamic model. Both models are closely coupled and a geometrically nonlinear aeroelastic solution is obtained by using load control and the Newton-Raphson root finding method. All analyses are performed at a trimmed flight condition, thus providing a fair comparison of the performance of different composite wings in the optimisation framework.

Finally, in the fourth module, the analysis results are processed and the output is generated. The module provides the deformed wing geometry and aeroelastic loads. Furthermore, from the beam deformation, the cross-sectional modeller can be used to compute the skin strains and assess the structural performance of the wing

3 OPTIMISATION PROCEDURE

In order to show the potential benefits of aeroelastic tailoring for manoeuvre load alleviation, several optimisations were run. The objective of the optimisation was to minimise the root bending moment of the wing under manoeuvre load conditions. The load cases that were run are shown in Table 1. Constraints were put on the maximum skin strains and the trim angle of attack to ensure a feasible structural design and to ensure linear aerodynamics and thus the validity of the aerodynamic model. For manufacturing purposes, all composite laminates have a fixed skin thickness and their layup is symmetric to prevent any warping upon curing. The composite laminates are described by lamination parameters to convert the inherently discrete composite optimisation problem into a continuous optimisation problem, thus allowing the use of a gradient based optimiser. Lamination parameters have the advantage that, when a symmetric laminate with a fixed number of layers is assumed, any laminate can be described by only 8 parameters thus also reducing the number of design variables compared to the case where each ply would be included as design variable. Note that, the disadvantage of lamination parameters is that they only provide a theoretical optimum, since they can only be matched exactly by an infinite number of layers. Some loss in performance of the wing is to be expected when these lamination parameters are converted to actual laminate; however the optimisation provides a good starting point to find the actual laminates that provide optimal performance. The sensitivities of the objective and constraints to the lamination parameters are computed analytically and the globally convergent method of moving asymptotes [23] was used as the optimiser.

Load case	#1	#2	#3
Flight speed [m/s]	100	100	100
Density [kg/m^3]	1.225	1.225	1.225
Load factor []	1	2.5	-1
Aircraft weight [kg]	56	56	56
Wing lift [N]	274.7	686.7	-274.7

Table 1: Manoeuvre load cases

4 DESIGN OF THE WINGS

The flight conditions and dimensions for which the wings are designed are shown in Table 1 and Table 2 respectively. The flight conditions and dimensions are based on the limitations of the low turbulence wind tunnel in which the wings will be tested. A wing with an aspect ratio of 10 was selected to test a wing representative for typical aircraft wings. Wing designs were made for three different cases, quasi isotropic (QI), constant stiffness (CS), and variable stiffness (VS). The quasi isotropic wing was build and analysed as a reference to be able to assess the potential benefits of the constant stiffness and variable stiffness wings. In case of constant stiffness, the wing is designed with a constant laminate along the span; a distinction is made only between the top and bottom skin. In case of variable stiffness, the wing is split into three equal spanwise sections, where each section has its own laminate for the top and bottom skin. In this way a preliminary assessment of the benefits of variable stiffness wings compared to constant stiffness wings can be made. The wings are made out of CYCOM 977-2-35 12k HTS carbon fibre epoxy with the material properties as shown in Table 3.

The result of the optimisation will be discussed in section 4.1, followed by the actual wing designs in section 4.2.

Semispan [m]	1
Chord [m]	0.2
Aspect ratio []	10
Sweep angle [deg]	0
Taper ratio []	1
Airfoil	NACA0012

Table 2: Test wing geometry

Material	CYCOM 977-2-35 12k HTS	Expanded Polypropylene (EPP)
E_{11} [GPa]	125.93[1]	9.8
E_{22} [GPa]	7.72[1]	9.8
G_{12} [GPa]	3.61[2]	3.77[3]
ν_{12} []	0.336[1]	0.3[4]
ρ [kg/m^3]	1590	20
t_{ply} [mm]	0.27	-

[1] according to ASTM Standard D3039
[2] according to ASTM Standard D3518
[3] according to $G = \frac{E}{2(1+\nu)}$
[4] assumed

Table 3: Material properties

4.1 Optimisation results

The results of the optimisation studies are shown in Table 4. Note that, expectedly, the critical load case for all wings was the 2.5g manoeuvre load, so analysis results are only presented for this load case. Initially, optimisations were run for 6 layers, since this is the smallest number of layers for which a quasi-isotropic wing ($[60/0/-60]_s$) can be manufactured. As can be seen, only a minor difference is found between the constant stiffness and variable stiffness wings and, as the results in section 4.2 show, this difference becomes even smaller when the lamination parameters are converted to the actual laminates. Therefore, extra optimisations were run for 3 and 4 layers, to amplify the benefit of a variable stiffness wing over a constant stiffness wing if the wing is allowed to deform more. For these wings no experimental comparison with an equivalent quasi-isotropic wing is possible; however, by making use of lamination parameters, the equivalent quasi-isotropic wing can still be analysed and these results provide an indication of the benefit of aeroelastic tailoring for 3 and 4 layers.

4.2 Actual wing designs

As mentioned before, the result of the optimisation is a set of lamination parameters. These lamination parameters have to be converted to actual laminates such that the wings can be manufactured. Therefore a sweep over the ply angles was done to find the laminate that best matches the optimum lamination parameters. Therewith a laminate that provides the largest reduction in root bending moment was found, while all the manufacturing constraints were still satisfied. Next an analysis using these laminates was run and by slightly changing the angles manually, the quality of the solution was investigated to see whether a slightly different laminate might result in improved performance and thus better design. For ease of manufacturing the same laminates were selected for the top and bottom skin, resulting in a symmetric wing about the chord.

Table 4 shows the results of the analysis of the actual results. As can be seen some performance is lost, but the actual laminates still show the clear benefit of aeroelastic tailoring for manoeuvre load reduction. The corresponding laminates can be found in Table 5. As can be seen and is also expected from literature [1], favourable bending-torsion coupling is introduced by orienting the fibres forward thus introducing negative twist upon deflection and shifting lift inboard. Note that observed bending-torsion coupling on the wing level is not introduced by bending-torsion coupling of the skin laminates. It is introduced by the skin extension-shear coupling instead. By applying positive loads the top skin will be in

compression, and the bottom skin will be in tension. Hence both skins will shear in opposite direction. By constraining shear deformation of the individual skin a wing twist is introduced. Inspecting the laminates and the corresponding root bending moment results, first of all, it is clear that the quasi-isotropic wings clearly have the highest root bending moment, since they have no bending-torsion coupling. Secondly, when comparing the constant stiffness wings to the variable stiffness wings, it is clear that in case of the variable stiffness wings, the root section is stiffer thus attracting more lift, while the tip section is more flexible thus having a higher favourable bending-torsion coupling and thus generating less lift. Consequently this will shift the lift inboard and thus a smaller root bending moment is obtained when compared to the constant stiffness wings.

Wing type		Root bending moment [Nm]			
		Optimised		Actual Laminates	
6 layers	QI	313.3		313.3	
	CS	295.6	-5.65%	295.5	-5.68%
	VS	295.2	-5.78%	295.2	-5.78
4 layers	QI	313.8		313.8	
	CS	293.2	-6.57%	293.9	-6.33%
	VS	290.9	-7.31%	291.9	-6.98%
3 layers	QI	313.6		313.6	
	CS	293.1	-6.54%	294.8	-5.99%
	VS	288.0	-8.16%	289.1	-7.81%

Table 4: Root bending moment results for a 2.5g load case for optimised and converted actual laminates

Wing type		Laminates (root to tip)		
6 layers	QI	$[60/0/-60]_s$		
	CS	$[30/87/30]_s$		
	VS	$[30/87/30]_s$	$[30/90/30]_s$	$[30/90/30]_s$
4 layers	CS	$[18/84]_s$		
	VS	$[17/88]_s$	$[34/83]_s$	$[21/42]_s$
3 layers	CS	[16/60/16]		
	VS	[30/8/30]	[30/90/30]	[30/90/30]

Table 5: Wing laminates. The ply angle is defined positive when the fibres are oriented forward when going from root to tip.

In order to prevent buckling and flattening of the cross-section under deflection, the initial wings of 3 and 6 layers had 20mm wide ribs made out of EPP (the material properties can be found in Table 3). When performing static tests, it turned out that the 3 layer wings buckled. Therefore, a FEM buckling analysis of the 4 layer wings was done in ABAQUS with an equivalent tip load of 200 N to simulate a similar deflection as is expected in the static test and wind tunnel experiments. As can be seen from the results in Table 6, for a rib spacing of 10 cm the EPP still does not provide sufficient support to prevent skin buckling and therefore

the 4 layer wings were filled with EPP completely resulting in a sufficient resistance to buckling, while only reducing the expected tip deflection by 4.9%. Although the EPP core was not taken into account in the aeroelastic modelling of the wings, a small reduction in the tip deflection and thus bending-torsion coupling is expected to have only a minor effect on the load alleviation results. Therefore a good correlation between analysis and test results is still expected.

Case	No ribs	Rib spacing 10 cm	Full core
Static load [N]	200	200	200
Buckling load [N]	58.3	68.9	547.76
Tip deflection [mm]	60.8	60.7	57.8

Table 6: Buckling load and tip deflection for various wing core configurations

5 EXPERIMENTS

Wing models were manufactured in the composite lab and tested in the low turbulence wind tunnel of TU Delft. The following sections present the manufacturing process and the experimental setup in more detail.

5.1 Manufacturing

In order to ensure high geometrical accuracy and high quality surface finish, the wings were manufactured using a hand-layup moulding technique. Several different wings had to be manufactured therefore the mould had to be robust enough to withstand several manufacturing cycles without any noticeable deterioration of the geometrical accuracy or surface finish quality. Furthermore, the mould had to be able to withstand high temperatures, since unidirectional carbon fibre prepreg was used which had to be cured in the autoclave at elevated temperature and pressure. Therefore a female mould was CNC milled out of aluminium.

The manufacturing procedure consisted of the following steps. First the prepreg tape was cut into quadrilateral patches according to individual ply-orientation requirements. This way the correct orientation of the fibres in the layup was ensured. After all the material had been stacked into the mould, the acquired layup was vacuum-bagged and cured in the autoclave. The cured skins had to be trimmed down to final size. Skin thickness was then measured and used as an offset to airfoil thickness for manufacturing the EPP ribs and cores. The EPP foam was cut using a CNC hot-wire cutting machine. Individual components before final assembly and the final assembly of the wing are shown in Figure 2 and 3, respectively.

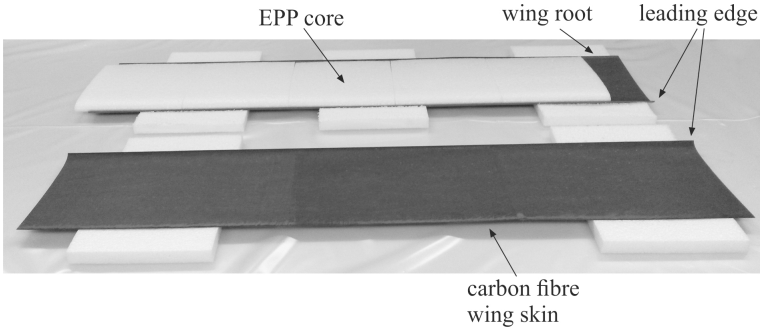

Figure 2: Wing components before assembly

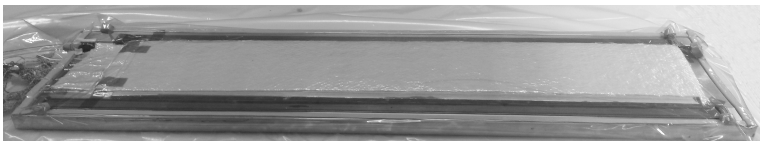

Figure 3: Vacuum bagging of the assembled wings to ensure proper bonding of both wing halves

5.2 Test setup

The performed tests were focused at static load alleviation. Therefore aerodynamic forces in terms of aerodynamic force and moment vector were measured by a mechanical six-component balance. Aerodynamic data was later reduced to lift and root bending moment coefficient.

Wing deformation in terms of deflections was measured by two independent methods: a VIC3D stereo digital image correlation system and an optical marker tracking system. VIC3D yields the 3D deformation field of the entire wing surface. Consequently, the acquired data had to be reduced to the quarter-chord line deflection and wing washout along the span. A DIC test setup and a wing painted with a speckle pattern are shown in Figure 4.

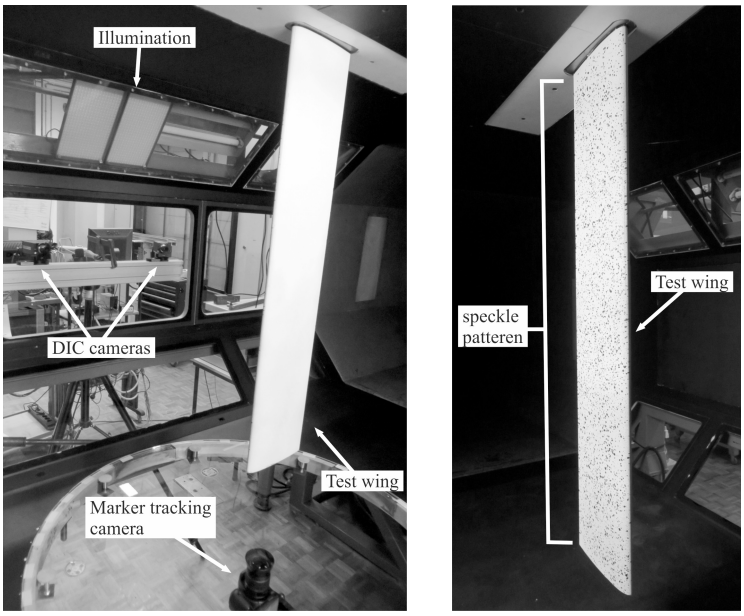

Figure 4: a) DIC test setup and b) test wing with a speckle pattern

Marker tracking was carried out by using a camera oriented along the span axis observing the wing tip. A set of distinctive markers were pasted on the wing tip. During the experiment the markers were photographed, however, their position was determined later, during the postprocessing of the measurements, using Matlab®. Due to its simplicity, marker tracking could be used to track the displacement and rotation of the wing tip only. Moreover it provided a redundant measurement in order to evaluate the quality of the VIC3D system. A set of captured frames with the recognized markers is shown in Figure 5. The position and orientation of the camera with respect to the wing is shown in Figure 4.

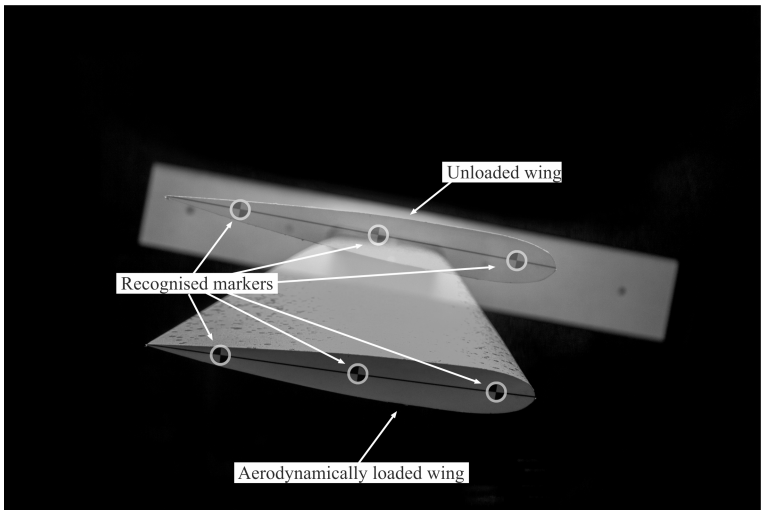

Figure 5: Overlay tip frames of unloaded and loaded ($\alpha_0 = 10°$ and $v_0 = 80$ m/s) CS 4 layer wing with recognised markers

6 RESULTS

Numerical and experimental results are presented for the QI six layer wing, to act as a reference, and for the CS and VS four layer wings, since these showed the largest reduction in root bending moment. In the remainder of the paper, these wings are referred to as QI, CS, and VS, respectively. First the aerodynamic results are presented, followed by a comparison of the structural deformations.

6.1 Lift and root bending moment coefficient

All the wings were tested at a range of free stream velocities from $v_0 = 10\,\mathrm{m/s}$ up to $v_0 = 100\,\mathrm{m/s}$ and at a range of incidence angles from $\alpha_0 = -10°$ up to $\alpha_0 = 10°$. Due to the qualitatively similar behaviour only the results corresponding to $v_0 = 40\,\mathrm{m/s}$, $60\,\mathrm{m/s}$ and $80\,\mathrm{m/s}$ with the respective Reynolds number of 0.54, 0.84 and $1.06 \cdot 10^6$, for all test wings are presented here.

A comparison between numerical and experiment results for the lift and root bending moment coefficient, C_L and C_M, of the QI, CS and VS wings are shown in Figure 6, 7 and 8, respectively. The comparison yields good agreement between numerical and experimental results. The average absolute difference in C_L with its respective deviation was $(7.2\%, 5{,}2\%)$, $(6.0\%, 7.5\%)$ and $(7.5\%, 8.3\%)$ for QI, CS and VS wing respectively. In the case of the C_M the numeric analysis tends to underpredict the coefficient value. The observed average absolute difference with its respective deviation was $(5.0\%,\ 5.3\%)$, $(10.3\%, 7.7\%)$ and $(10.8\%, 9.4\%)$ for the QI, CS and VS wing respectively.

Comparison between the tested wings reveals significant effect of the aeroelastic tailoring on the wing aerodynamic properties. The dependence of C_L and C_M on the free stream velocity is negligible in the case of the QI wing. On the other hand, in the case of the CS and VS wing, one can clearly observe that the $\partial C_L/\partial \alpha_0$ and $\partial C_M/\partial \alpha_0$ are decreasing as the v_0 is increased. The phenomenon can be explained by the increasing washout of the wing tip as the aerodynamic loads increase. Consequently the wing passively alleviates the overall loads which results in lower measured C_L and C_M values. The washout is caused by the bending-torsion coupling of the wing structure which is governed by the extension-shear coupling on the wing skin level. In turn the behaviour of the QI wing can be explained by the absence of

such bending-torsion coupling which is consistent with the expectations outlined in section 4. It is important to point out that the measurements validate the numerical predictions.

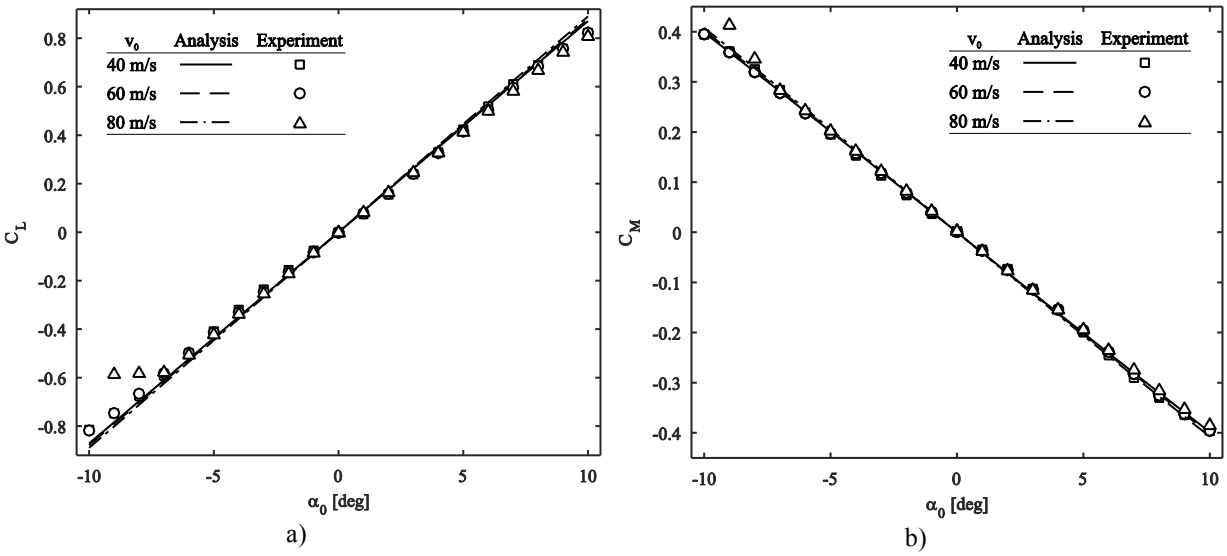

Figure 6: a) Lift and b) root bending moment coefficient of the QI wing

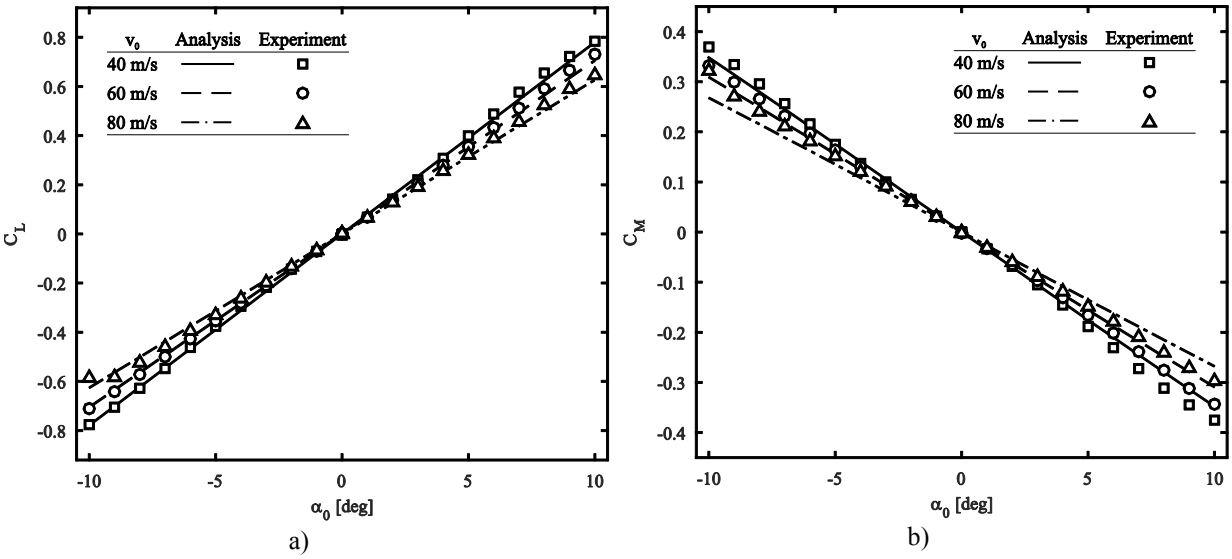

Figure 7: a) Lift and b) root bending moment coefficient of the CS wing

Aerodynamic performance of the VS wing differs only marginally from that of the CS wing as can be observed in Figure 9. Obviously the additional degrees of freedom in the VS wing laminate design did not yield significant design improvement. That however asserts the design results shown in Table 4 which also yielded only a 10% improvement due to the variable stiffness skin design. That means that the approach to variable stiffness tailoring should be reconsidered in order to better exploit its potential. It is noteworthy that currently variable stiffness was reduced to three different constant stiffness sections and that the number of plies comprising the laminate was rather limited which considerably hinders the conversion from the lamination parameters to the actual laminate. These aspects however remain to be investigated both numerically and experimentally in the future.

Final remark regarding the aerodynamic results is concerned with the QI's lift coefficient. At $v_0 = 80\ \mathrm{m/s}$ and $\alpha_0 \leq -8°$ the C_L stagnates roughly at value of -0.6 which is attributed to

the structural instability of the wing under the exerted aerodynamic loads which led to unpredictable change in wing shape. This is discussed in more detail in section 6.2.

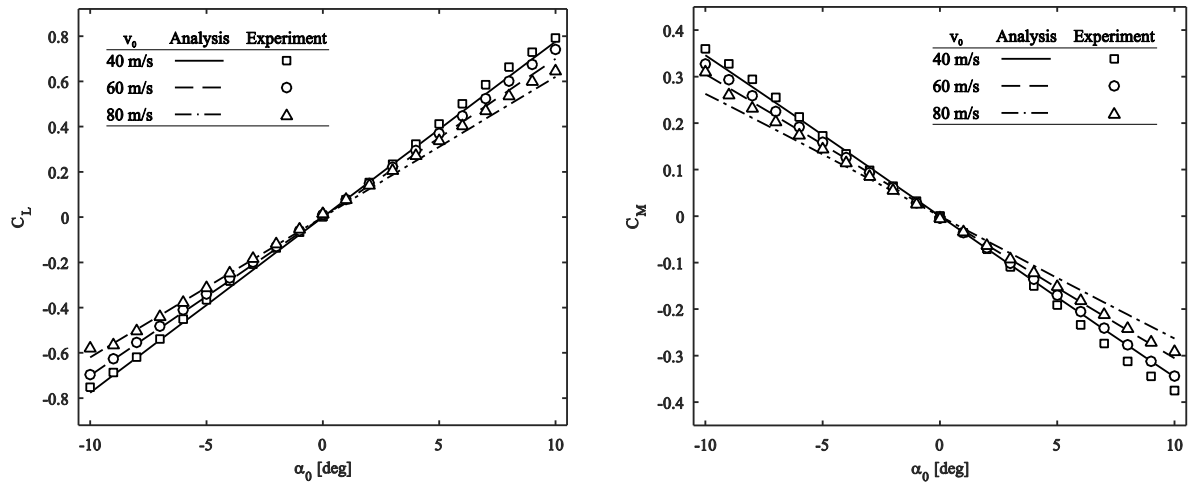

Figure 8: a) Lift and b) root bending moment coefficient of the VS wing

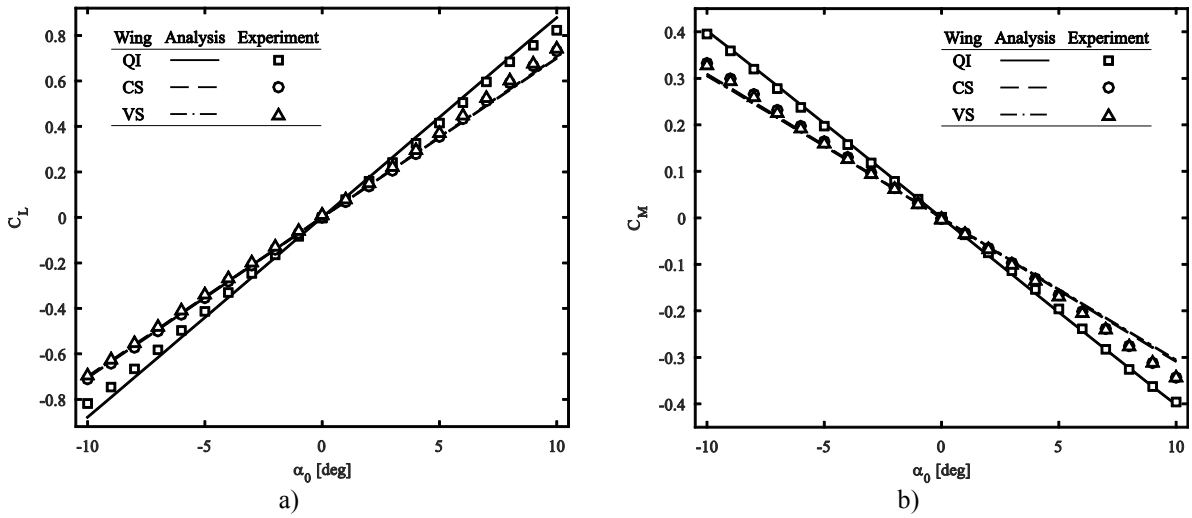

Figure 9: Comparison between QI, CS and VS wings at $v_0 = 60$ m/s: a) lift coefficient and b) root bending moment coefficient

6.2 Wing deformation

It is important to point out that the DIC was actually measuring the deformation of the wing skin rather than the deformation of the wing's beam axis directly. Hence additional postprocessing was required in order to correlate the measured deformations to the predicted deformations obtained by the numerical analysis. Despite the postprocessing some artefacts pertinent to the skin deformation remain in the DIC results. The most noticeable is the waviness of the DIC quarter-chord line near the wing's root. However, measuring the skin deformation turned out to be very valuable during the experiments, since the onset of structural instability could be easily detected. Moreover it helps to clearly identify the instability mode as well.

Both DIC and marker tracking measurements show very good agreement with the numerical results for all the load cases below the onset of structural instability. The average absolute

difference with the corresponding deviation in case of the out-of-plane tip displacement was $(3.2\%, 8.3\%)$, $(2.6\%, 5.7\%)$ and $(2.3\%, 5.0\%)$ for the QI, CS and VS wing respectively. Structural instability, in particular buckling analysis of individual components comprising the wing has not been included in the analysis tool. Thus, a worse prediction can be expected when buckling occurs.

From the tested wings the QI wing tends to buckle first, despite having the thickest laminate. Such outcome is explained by the difference in the inner structure of the wings. The QI wing skin was supported only by four EPP foam ribs equally spaced along the span from root to tip. On the other hand the CS and VS wing contained a continuous EPP core supporting the wing skins over the entire span. It is noteworthy that the numerical analysis did not account for the effect of the foam on the bending properties of the wing. It was assumed that the effect was negligible due to the relatively low stiffness properties of the EPP foam. The Young's modulus of EPP is an order of magnitude smaller than the primary stiffness of the used carbon fibre prepreg. The results shown in Figure 10, 11 and 12 indeed assert the validity of the assumption.

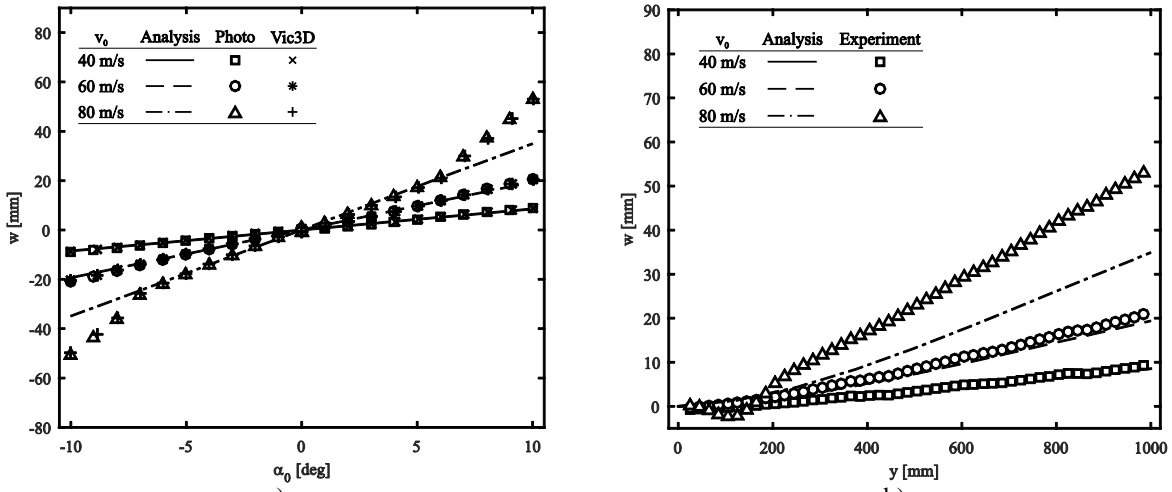

Figure 10: a) QI out-of-plane tip deflection at α_0 and b) QI out-of-plane deflection of the quarter-chord line at $\alpha_0 = 10°$

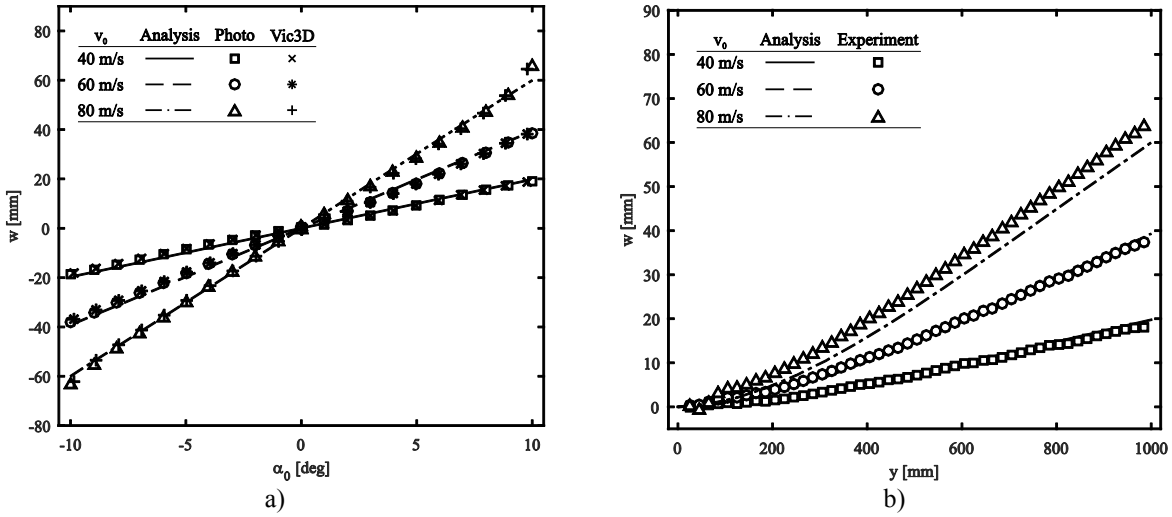

Figure 11: CS out-of-plane tip deflection at α_0 and b) CS out-of-plane deflection of the quarter-chord line at $\alpha_0 = 10°$

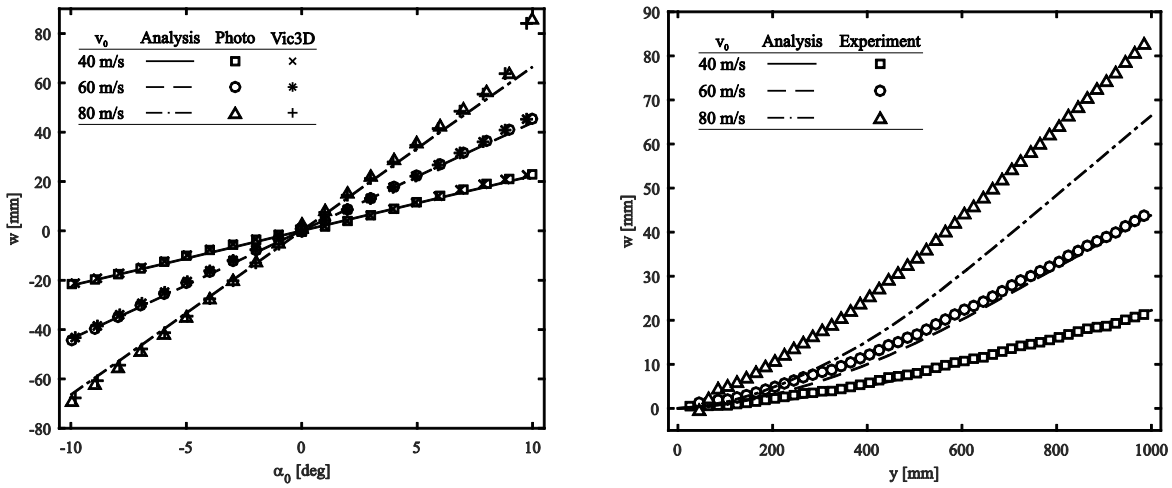

a) b)

Figure 12: VS out-of-plane tip deflection at α_0 and b) VS out-of-plane deflection of the quarter-chord line at $\alpha_0 = 10°$

A direct comparison between the tested wings at $v_0 = 60\ \mathrm{m/s}$ and $\alpha_0 = 10°$ is shown in Figure 13. Due to substantial difference in layup stiffness the QI wing exhibits much lower level of deformation than the CS and VS wings which are, from a structural point of view, more comparable to each other. Interestingly, the CS and VS aerodynamic performance, both numerical and experimental, were almost identical, however there are some noticeable differences between the two wings in the structural behaviour. According to results shown in Figure 13a, the VS wing is more compliant than the CS wing. Upon inspection of the quarter-chord line deflections shown in Figure 13b one can observe that near the root the two wings behave similarly however near the tip region, the VS wing is considerably more compliant than the CS wing. Such behaviour is expected since the two wings were designed for maximum passive root bending moment alleviation. Laminate tension-shear coupling on the skin level is exploited to induce washout on the wing level, therewith shifting the aerodynamic loads towards the root of the wing. The amount of washout induced by the tension-shear coupling is proportional to the induced shear strains. In the case of the CS wing the same laminate was used along the span, hence the design procedure has to find a balance between the stiffness of the whole wing and the amount of tension-shear coupling present in the laminate. On the other hand, in the case of the VS wing the laminate in the root section could be different than the laminate in the tip section having different stiffness and coupling properties. The outboard section of the wing is hence designed more compliant which eventually results in higher tip deflections of the VS wing.

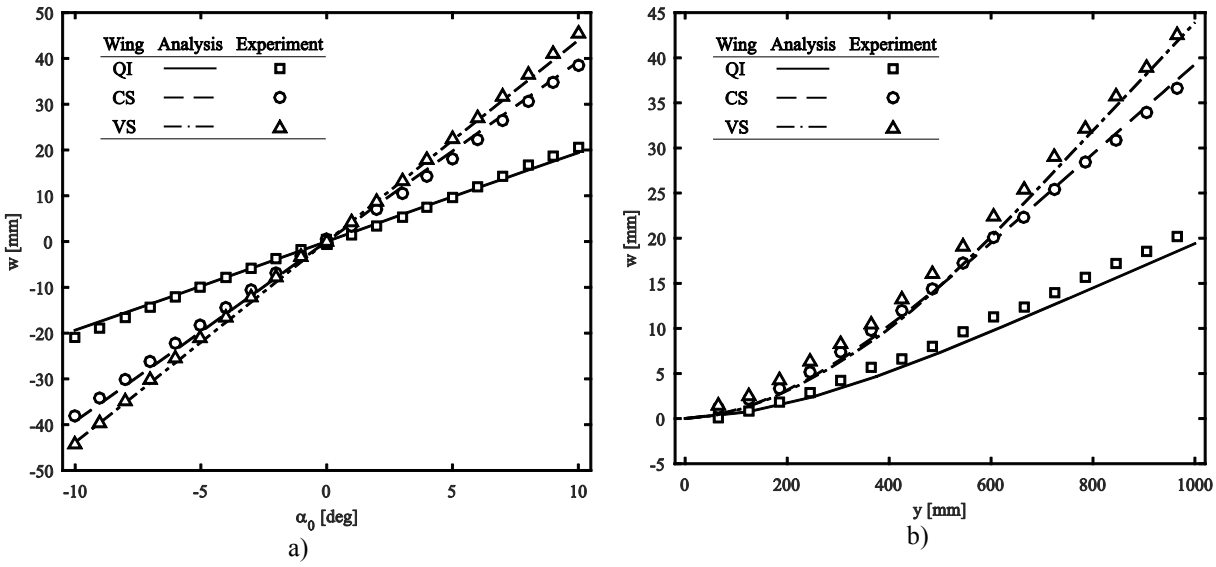

Figure 13: Comparison between QI, CS and VS wings at $v_0 = 60$ m/s: a) out-of-plane tip deflection and b) out-of plane deflection of the quarter-chord line at $\alpha_0 = 10°$

7 CONCLUSION

A successful implementation of the aeroelastic analysis into a gradient-based design routine was demonstrated. The design routine was later successfully applied to the composite layup optimisation for root bending moment alleviation of flexible composite wing.

In order to improve our understanding of the material tailoring effect on the aeroelastic properties of wings, two layups, a constant and a variable stiffness, were devised and a set of carbon fibre-epoxy aeroelastically tailored wings were manufactured. In addition to the constant and variable stiffness wings, a quasi-isotropic wing was manufactured as well which served as a reference wing exhibiting no tailoring effects.

A static aeroelastic experiment was performed in the TU Delft LTT wind tunnel. During the aeroelastic experiment, the aerodynamic force and moment vector were measured using a six component balance. Moreover, two digital image correlation systems were used to measure the wing's deformation.

Numeric and experimental data was compared to each other. It can be concluded that the numeric results match the experimental data very well for all the load cases below the onset of structural instability of the wings. In the case of the lift and root bending moment coefficient the difference is less than 10%, while the difference in the case of out-of-plane deflection is below 3.2%. The discrepancy between the two data sets gets larger as the wings start to buckle which can be expected, since the numerical analysis does not account for such phenomena.

Experimental data show that both constant and variable stiffness wing behave according to numerical predictions. In comparison to quasi-isotropic wing these wings exhibit significant effect of aeroelastic tailoring on all the measured quantities. Moreover, there is also a noticeable difference between the two tailored wings. The difference is visible in the tip and the quarter-chord line out-of-plane deflection. However the difference in terms of lift and root-bending moment coefficient between the two wings could not be experimentally confirmed.

EPP foam core used to support the wing skin has a negligible effect on the wing bending stiffness. However its effect on the skin buckling is very strong. The quasi-isotropic wing which contained only discrete foam ribs buckled first despite it having the stiffest and thickest skin, while the other two wings had considerably thinner and more compliant carbon fibre skins but were built with an EPP core spanning the entire wing.

8 ACKNOWLEDGEMENT

The authors would like to thank Peter Loeffen for his help with building and preliminary static testing of the presented tailored composite wings.

9 REFERENCES

[1] M. H. Shirk, T. J. Hertz, and T. A. Weisshaar, "Aeroelastic tailoring - Theory, practice, and promise," *J. Aircr.*, vol. 23, no. 1, pp. 6–18, 1986.

[2] Z. Qin, P. Marzocca, and L. Librescu, "Aeroelastic instability and response of advanced aircraft wings at subsonic flight speeds," *Aerosp. Sci. Technol.*, vol. 6, no. 3, pp. 195–208, Mar. 2002.

[3] Z. Qin, L. Librescu, and P. Marzocca, "Aeroelasticity of composite aerovehicle wings in supersonic flows," *J. Spacecr. Rockets*, vol. 40, no. 2, pp. 162–173, 2003.

[4] T. A. Weisshaar, "Aeroelastic tailoring - Creative uses of unusual materials," 1987.

[5] A. Danilin and T. Weisshaar, "The use of structural optimality criteria for aircraft conceptual design," in *41st Structures, Structural Dynamics, and Materials Conference and Exhibit*, American Institute of Aeronautics and Astronautics.

[6] Eli Livne and T. Weisshaar, "Aeroelasticity of Nonconventional Airplane Configurations - Past and Future," *J. Aircr. - J Aircr.*, vol. 40, no. 6, pp. 1047–1065, 2003.

[7] T. A. Weisshaar and D. K. Duke, "Induced Drag Reduction Using Aeroelastic Tailoring with Adaptive Control Surfaces," *J. Aircr.*, vol. 43, no. 1, pp. 157–164, 2006.

[8] F. E. Eastep, V. A. Tischler, V. B. Venkayya, and N. S. Khot, "Aeroelastic Tailoring of Composite Structures," *J. Aircr.*, vol. 36, no. 6, pp. 1041–1047, 1999.

[9] H. Arizono and K. Isogai, "Application of Genetic Algorithm for Aeroelastic Tailoring of a Cranked-Arrow Wing," *J. Aircr.*, vol. 42, no. 2, pp. 493–499, 2005.

[10] S. J. Guo, J. R. Bannerjee, and C. W. Cheung, "The effect of laminate lay-up on the flutter speed of composite wings," *Proc. Inst. Mech. Eng. Part G J. Aerosp. Eng.*, vol. 217, no. 3, pp. 115–122, 2003.

[11] S. Guo, W. Cheng, and D. Cui, "Optimization of composite wing structures for maximum flutter speed," presented at the Collection of Technical Papers - AIAA/ASME/ASCE/AHS/ASC Structures, Structural Dynamics and Materials Conference, 2005, vol. 6, pp. 4091–4100.

[12] J. Dillinger, M. M. Abdalla, T. Klimmek, and Z. Gürdal, "Static aeroelastic stiffness optimization and investigation of forward swept composite wings," in *10th World Congress on Structural and Multidisciplinary Optimization*, 2013, pp. 19–24.

[13] S. Guo, W. Cheng, and D. Cui, "Aeroelastic tailoring of composite wing structures by laminate layup optimization," *AIAA J.*, vol. 44, no. 12, pp. 3146–3150, 2006.

[14] M. Kameyama and H. Fukunaga, "Optimum design of composite plate wings for aeroelastic characteristics using lamination parameters," *Comput. Struct.*, vol. 85, no. 3–4, pp. 213–224, 2007.

[15] A. Manan, G. A. Vio, M. Y. Harmin, and J. E. Cooper, "Optimization of aeroelastic composite structures using evolutionary algorithms," *Eng. Optim.*, vol. 42, no. 2, pp. 171–184, 2010.
[16] D. M. De Leon, C. E. De Souza, J. S. O. Fonseca, and R. G. A. Da Silva, "Aeroelastic tailoring using fiber orientation and topology optimization," *Struct. Multidiscip. Optim.*, vol. 46, no. 5, pp. 663–677, 2012.
[17] C. L. Pettit and R. V. Grandhi, "Optimization of a wing structure for gust response and aileron effectiveness," *J. Aircr.*, vol. 40, no. 6, pp. 1185–1191, 2003.
[18] T.-U. Kim and I. H. Hwang, "Optimal design of composite wing subjected to gust loads," *Comput. Struct.*, vol. 83, no. 19–20, pp. 1546–1554, 2005.
[19] O. Stodieck, J. E. Cooper, P. M. Weaver, and P. Kealy, "Improved aeroelastic tailoring using tow-steered composites," *Compos. Struct.*, vol. 106, pp. 703–715, 2013.
[20] G. A. A. Thuwis, R. De Breuker, M. M. Abdalla, and Z. Gürdal, "Aeroelastic tailoring using lamination parameters :Drag reduction of a Formula One rear wing," *Struct. Multidiscip. Optim.*, vol. 41, no. 4, pp. 637–646, 2010.
[21] N. P. M. Werter and R. De Breuker, "Aeroelastic tailoring and structural optimisation using an advanced dynamic aeroelastic framework," presented at the International Forum on Aeroelasticity and Structural Dynamics 2015, Saint Petersburg.
[22] E. A. Ferede and M. M. Abdalla, "Cross-sectional modelling of thin-walled composite beams," presented at the 55th AIAA/ASMe/ASCE/AHS/SC Structures, Structural Dynamics, and Materials Conference, 2014.
[23] K. Svanberg, "A class of globally convergent optimization methods based on conservative convex separable approximations," *SIAM J. Optim.*, vol. 12, no. 2, pp. 555–573, 2002.

10 COPYRIGHT STATEMENT